IUGR with infantile overnutrition programs an insulin-resistant phenotype through DNA methylation of *peroxisome proliferator–activated receptor-γcoactivator-1α* in rats

Xuemei Xie[1], Tulian Lin[1], Meihui Zhang[1], Lihong Liao[1], Guandou Yuan[2], Hongjie Gao[1], Qin Ning[3] and Xiaoping Luo[1]

BACKGROUND: Intrauterine growth restriction (IUGR) followed by postnatal accelerated growth (CG-IUGR) is associated with long-term adverse metabolic consequences, and an involvement of epigenetic dysregulation has been implicated. Peroxisome proliferator–activated receptor-γ coactivator-1α (PGC-1α) is a key orchestrator in energy homeostasis. We hypothesized that CG-IUGR programed an insulin-resistant phenotype through the alteration in DNA methylation and transcriptional activity of PGC-1α.

METHODS: A CG-IUGR rat model was adopted using maternal gestational nutritional restriction followed by infantile overnutrition achieved by reducing the litter size. The DNA methylation was determined by pyrosequencing. The mRNA expression and mitochondrial content were assessed by real-time PCR. The insulin-signaling protein expression was evaluated by western blotting.

RESULTS: Compared with controls, the CG-IUGR rats showed an increase in the DNA methylation of specific CpG sites in PGC-1α, and a decrease in the transcriptional activity of PGC-1α, mitochondrial content, protein level of PI3K and phosphorylated-Akt2 in liver and muscle tissues. The methylation of specific CpG sites in PGC-1α was positively correlated with fasting insulin concentration.

CONCLUSION: IUGR followed by infantile overnutrition programs an insulin-resistant phenotype, possibly through the alteration in DNA methylation and transcriptional activity of PGC-1α. The genetic and epigenetic modifications of PGC-1α provide a potential mechanism linking early-life nutrition insult to long-term metabolic disease susceptibilities.

Early-life environment plays a critical role in long-term health and diseases. The environmental insults during pivotal periods of development probably trigger maladaptive alterations in organism structure and function, contributing to metabolic syndrome (1), type II diabetes (T2DM) (2), and cardiovascular disease (3) in later life.

It has been well documented that low birth weight is associated with long-term disadvantageous metabolic consequences (1,2,4–7). Many intrauterine growth restriction (IUGR) infants experience postnatal accelerated growth (8), begetting short-term (9) and long-term health benefits, especially in cognition and academic achievement (10). However, emerging evidence suggests that IUGR followed by postnatal accelerated growth (CG-IUGR) plays a role in the programing of adult metabolic disease risk (11–13), and the underlying molecular pathogenesis is unclear. Nevertheless, the epigenetic dysregulation has been implicated. Paradoxically, in a few studies, catch-up growth may mitigate adult glucose intolerance (2,7).

Nutritional insults such as famine (14) or overfeeding (15) during crucial developmental stages may program later-life adverse metabolic consequences through epigenetic modifications such as DNA methylation. *Peroxisome proliferator–activated receptor-γcoactivator-1α* (*PGC-1α*) has emerged as a key orchestrator in energy homeostasis and metabolism, favorably regulating mitochondrial biogenesis and function (16). Highly responsive to environmental cues and abundantly expressed in skeletal muscle and liver, two insulin-sensitive organs, *PGC-1α* serves as a crucial node linking nutritional signals to energy metabolism (16). And, recently, the alteration of DNA methylation in *PGC-1α* promoter in liver and muscle has been associated with T2DM (17), nonalcoholic fatty liver disease (18), and high-fat consumption in a birth-weight-dependent manner (19) in human, inferring that epigenetic modification of *PGC-1α* is a potential molecular pathogenesis for insulin resistance-related disorders and probably plays a role in metabolic programing.

We previously demonstrated that rat offspring that suffer nutritional insults in fetal and weaning period develop aberrant growth trajectories and, as adults, an insulin-resistant phenotype including impaired insulin signaling (20–22). Insulin resistance has been considered as an early manifestation as well as a crucial mechanism for metabolic diseases such as T2DM in adults with CG-IUGR.

[1]Department of Pediatrics, Tongji Hospital, Tongji Medical College, Huazhong University of Science and Technology, Wuhan, China; [2]Hepatic Surgery Center, Tongji Hospital, Tongji Medical College, Huazhong University of Science and Technology, Wuhan, China; [3]Department of Infectious Diseases, Tongji Hospital, Tongji Medical College, Huazhong University of Science and Technology, Wuhan, China. Correspondence: Xiaoping Luo (xpluo@tjh.tjmu.edu.cn)

Received 22 June 2014; accepted 5 November 2014; advance online publication 11 March 2015. doi:10.1038/pr.2015.32

In this study, using a well-established rodent model, we explored the role of *PGC-1α* promoter methylation in programing the insulin-resistant phenotype arising from IUGR followed by infantile overnutrition. The DNA methylation level and transcriptional activity of *PGC-1α* in liver and skeletal muscle were quantified. Insofar as PGC-1α is a master regulator of mitochondrial biogenesis, the mitochondrial content and the transcriptional modifications of related genes were determined. The post-transcriptional alteration of the canonical components of insulin-signaling pathway was also evaluated to further identify the underpinning of metabolic programing via *PGC-1α* methylation. We chose to study offspring as young adults because the early postnatal accelerated growth has been achieved at this stage when insulin resistance manifests and epigenetic modifications have transpired.

RESULTS

CG-IUGR Model

In accordance with our previous studies (20–22), the IUGR pups had lower birth weights than normal control (appropriate for gestational age—AGA group) and caught up with the AGA pups prior to the third postnatal week; since then, the weights of the CG-IUGR rats kept increasing and were significantly higher than those of the AGA group at the third, fourth and eighth week (**Figure 1a**). Correspondingly, the BMI of the IUGR group were lower than those of the AGA group at birth, and surpassed the AGA group since the third week (**Figure 1b**).

Although the body weight was increased in adult CG-IUGR rats, the core body temperature and spontaneous physical activity, both of which could affect *PGC-1α* expression, were comparable between the two groups ($P > 0.05$, data not shown).

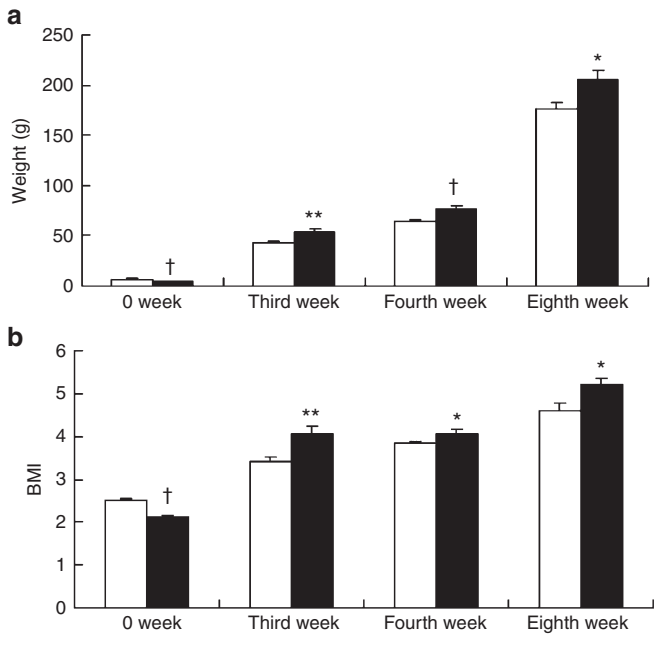

Figure 1. Intrauterine growth restriction (IUGR) with infantile overnutrition growth model. Body weight (**a**) and BMI (**b**) of control and CG-IUGR rats at birth, third, fourth, and eighth week. The black and white bars refer to CG-IUGR and normal control group, respectively. Data are presented as mean ± SEM ($n \geq 9$ for each group). *$P < 0.05$, **$P < 0.01$, †$P < 0.001$ compared with same-age controls.

DNA Methylation and PGC-1α mRNA Expression

The methylation level of specific CpG sites –787 and –803 of *PGC-1α* promoter in both liver and skeletal muscle of the CG-IUGR rats was higher than that of the AGA rats, while the methylation level of other CpG sites in PGC-1α promoter was comparable between groups (**Figure 2a,b**). The DNA methylation of gene promoter was implicated to inversely modulate the transcriptional activity (23). In accordance with the higher methylation level of CpG sites –787 and –803, the mRNA expression of *PGC-1α* was decreased in both the liver and muscle of CG-IUGR rats (**Figure 2c**). Interestingly, the DNA methylation level did not correlate significantly with the mRNA content of *PGC-1α* in liver ($r = -0.476$, $P = 0.139$ for CpG site –803; $r = -0.518$, $P = 0.103$ for CpG site –787) or in muscle ($r = -0.509$, $P = 0.162$ for CpG site –803; $r = -0.307$, $P = 0.421$ for CpG site –787)

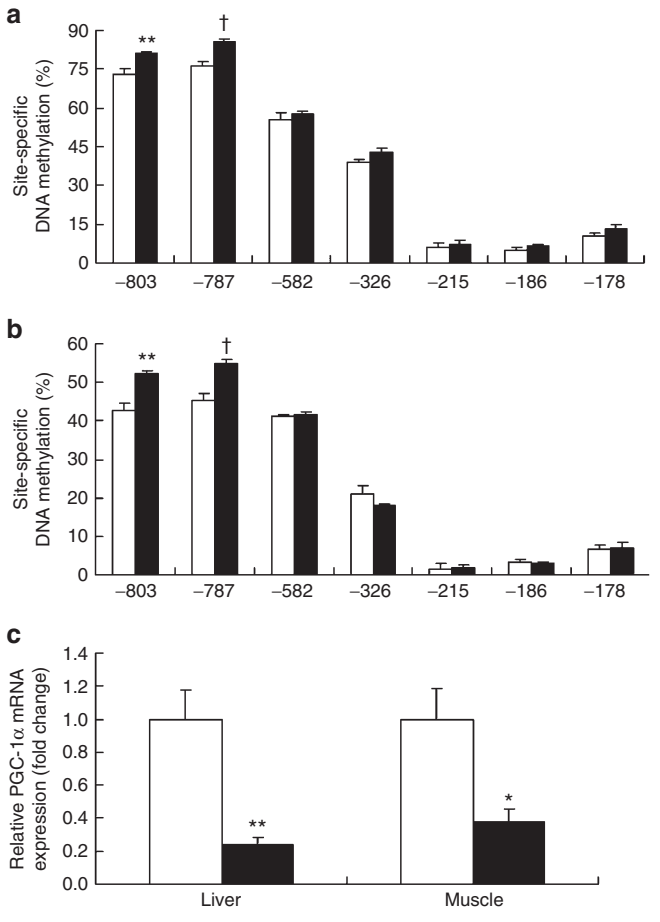

Figure 2. The DNA methylation and mRNA expression of *PGC-1α* in liver and muscle. The DNA methylation level of specific CpG sites of the *PGC-1α* promoter in liver (**a**) and muscle (**b**). (**c**) The relative mRNA expression of *PGC-1α* in liver and muscle was reduced in CG-IUGR rats. The black and white bars refer to CG-IUGR and normal control group, respectively. Data are presented as mean ± SEM ($n = 5–7$). *$P < 0.05$, **$P < 0.01$, †$P < 0.001$ compared with controls.

Mitochondrial Content

Compared with control, the ratio of mitochondrial DNA (mtDNA) to nucleus DNA (nDNA) was reduced, indicative of attenuated mitochondrial content in the liver and muscle of CG-IUGR rats (**Figure 3a**). Furthermore, the mtDNA/nDNA ratio was positively correlated with *PGC-1α* mRNA level ($r = 0.781$, $P = 0.008$), and inversely correlated with the methylation level of CpG site −787 ($r = -0.641$, $P = 0.033$) but not with that of CpG site −803 of *PGC-1α* promoter in liver; interestingly, in skeletal muscle, the mtDNA/nDNA ratio was inversely correlated with the methylation level of CpG site −787 ($r = -0.723$, $P = 0.012$) as well as CpG site −803 ($r = -0.823$, $P = 0.002$) of *PGC-1α* promoter, but was not correlated with *PGC-1α* mRNA level.

The transcription activities of *PGC-1α* target genes involved in mitochondrial respiratory chain including *cytochrome C (Cycs)*, *succinate dehydrogenase cytochrome b small subunit (Sdhd)*, *complex III subunit 1 (Uqcrc1)*, and *ATP synthase subunit beta (Atp5b)* were measured. The mRNA abundance of *Cycs*, *Sdhd*, and *Atp5b* was decreased in the liver of CG-IUGR group compared with that of the control, while the mRNA level of *Uqcrc1* was unchanged (**Figure 3b**). Interestingly, in muscle, the mRNA level of *Sdhd* and *Uqcrc1* was decreased in CG-IUGR rats whereas the mRNA level of *Cycs* and *Atp5b* was comparable between groups (**Figure 3c**).

Additionally, the mRNA expression of *mitochondrial transcription factor A (TFAM)* and *nuclear respiratory factors 1 (NRF1)*, two downstream transcription factors of PGC-1α known to regulate mitochondrial biogenesis (16), was investigated. The mRNA level of *NRF1* was attenuated in both the liver and muscle of CG-IUGR rats; interestingly, *TFAM* mRNA abundance was decreased in the muscle of CG-IUGR rats but was comparable in liver between the two groups (**Figure 3b**,**c**).

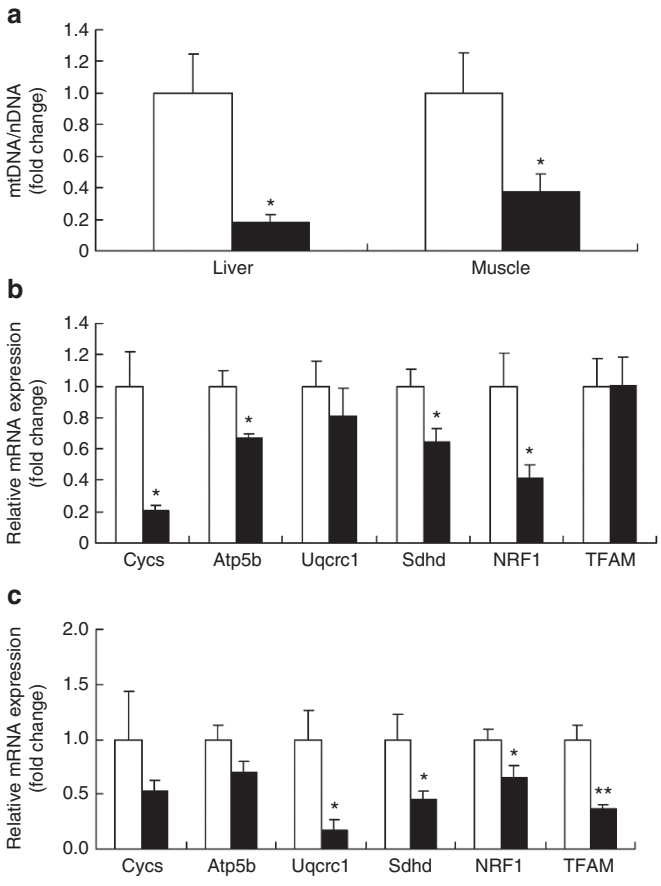

Figure 3. Mitochondrial content and mRNA abundances of other mitochondrial markers. (**a**) Decreased mitochondrial content (mtDNA/nDNA ratio) in liver and muscle of CG-IUGR rats. The relative mRNA abundances of PGC-1α target genes involved in oxidative phosphorylation in liver (**b**) and muscle (**c**). The black and white bars refer to CG-IUGR and normal control group, respectively. Data are presented as mean ± SEM ($n = 6$). *$P < 0.05$, **$P < 0.01$ compared with controls.

The mRNA Expression of PGC-1α Target Genes Involved in Fatty Acid Oxidation and Tissue Triglyceride (TG) Content

The mRNA expression of PGC-1α target genes involved in fatty acid oxidation, including *peroxisome proliferator–activated receptor-α* (*PPAR-α*), *carnitine palmitoyltransferase 1A* (*CPT1A*), *CPT1B*, *fatty acid translocase (FAT/CD36)*, as well as *PPAR-γ* was determined. The mRNA level of *PPAR-α* was attenuated while *CPT1A/CPT1B* was not changed in the liver/muscle tissue of CG-IUGR rats (**Figure 4a**,**b**). *CD36* and *PPAR-γ* mRNA contents were reduced in the liver of CG-IUGR rats but comparable in muscle between the groups (**Figure 4a**,**b**).

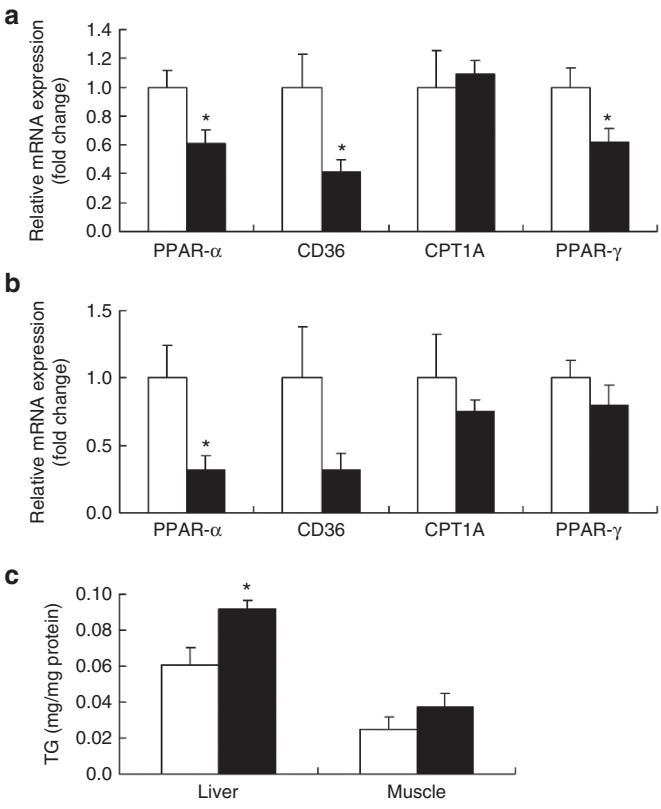

Figure 4. The mRNA expression of PGC-1α target genes involved in fatty acid oxidation in (**a**) liver and (**b**) muscle, and TG content (**c**) in rat liver and muscle tissues. The black and white bars refer to CG-IUGR and normal control group, respectively. Data are presented as mean ± SEM ($n = 5$–6). *$P < 0.05$ compared with controls.

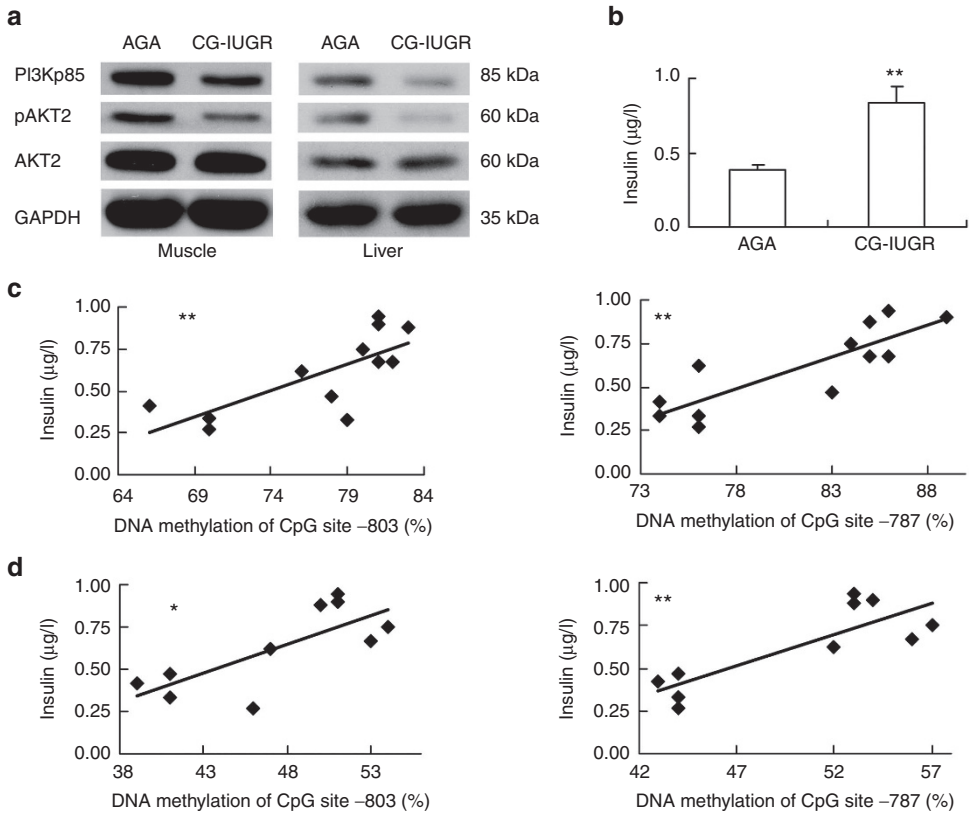

Figure 5. Impaired insulin signaling and increased fasting insulin level. (**a**) The protein content of key components in insulin-signaling pathway was reduced in the liver and muscle tissues of CG-IUGR rats ($n = 6$). (**b**) Fasting plasma insulin level was increased in CG-IUGR rats ($n = 8$). The insulin level was positively correlated with the methylation level of CpG sites –787 ($r = 0.843$, $P = 0.001$ for liver and $r = 0.833$, $P = 0.003$ for muscle) and –803 ($r = 0.741$, $P = 0.006$ for liver and $r = 0.756$, $P = 0.011$ for muscle) of *PGC-1α* promoter in liver (**c**) and muscle (**d**). Data are presented as mean ± SEM. *$P < 0.05$, **$P < 0.01$ compared with controls.

The TG content was higher in the liver tissue of CG-IUGR rats compared with that of the AGA group (Figure 4c). Moreover, the TG level was positively correlated with the methylation level of CpG sites –787 ($r = 0.680$, $P = 0.03$) and –803 ($r = 0.790$ and $P = 0.007$) of *PGC-1α* promoter in liver. Conversely, the TG content in skeletal muscle did not differ between the groups.

Insulin Signaling and Fasting Insulin Level

Consistent with our previous studies (21,22), the protein content of PI3K p85 as well as pS474-Akt2 was significantly reduced in the liver and muscle tissues of CG-IUGR rats (Figure 5a), indicative of impaired insulin signaling.

The fasting plasma insulin level was increased in CG-IUGR rats compared with AGA group (Figure 5b). Furthermore, insulin level was positively correlated with the methylation level of CpG sites –787 ($r = 0.843$, $P = 0.001$ for liver and $r = 0.833$, $P = 0.003$ for muscle) and –803 ($r = 0.741$, $P = 0.006$ for liver and $r = 0.756$, $P = 0.011$ for muscle) of *PGC-1α* promoter (Figure 5c,d). There was also a suggestion of correlation between insulin level and mtDNA/nDNA ratio in liver ($r = -0.571$, $P = 0.066$).

DISCUSSION

Numerous studies have concluded that IUGR individuals, especially those with postnatal accelerated growth, are prone to develop insulin resistance and T2DM in adulthood (11–13). Using a well-established rodent model, these experiments have found that CG-IUGR rats had higher methylation level of specific CpG sites of *PGC-1α* promoter, in contrast, reduced *PGC-1α* transcription activity, mitochondrial content as well as protein level of key components of insulin-signaling pathway in liver and muscle tissues. Consistent with our previous findings (20–22), the CG-IUGR young adult rats presented an insulin-resistant phenotype including higher BMI, impaired insulin signaling, and elevated fasting insulin level, indicative of a programing change arising from the adverse early-life nutritional exposure. Our previous studies found that CG-IUGR rats had normal fasting blood glucose concentration despite increased fasting insulin level (21,22).

Early nutritional insults may program long-term disease susceptibilities through epigenetic modification (14,15). Recently, the DNA methylation level of *PGC-1α* promoter in umbilical cord has been found to positively correlate with maternal pregestational BMI (24); moreover, the *PGC-1α* methylation level is increased in the muscle of low-birth-weight adults (19,25), and 5-d overfeeding may influence the DNA methylation of *PGC-1α* in a birth-weight-dependent manner (19); besides, maternal methyl donor-deficient diet leads to PGC-1α protein hypomethylation in the liver of the pups with subsequent impairment of fatty acid oxidation (26), suggesting that both

Figure 6. CpG sites investigated in *PGC-1α* promoter. The seven CpG sites analyzed are marked with a perpendicular line.

prenatal and postnatal nutritional status may play a crucial role in metabolic programing through the epigenetic modification of *PGC-1α*. In our study, the methylation level of CpG sites −787 and −803 of *PGC-1α* promoter was higher in the liver and muscle of CG-IUGR rats while the methylation level of other CpG sites was comparable between the groups, and the methylation level of specific CpG sites was positively correlated with fasting insulin level. The site-specific alteration of DNA methylation in the *PGC-1α* promoter infers that CpG sites −803 and −787 are more sensitive to nutritional cues, and may have a unique role in programing insulin sensitivity and metabolic disease susceptibilities in response to the uterine malnutrition (IUGR) followed by infantile overnutrition status (postnatal accelerated growth). Similarly, previous studies have demonstrated that *PGC-1α* promoter methylation level is increased in liver from patients with nonalcoholic fatty liver disease (18), as well as in islet (17) and skeletal muscle (27) from patiens with T2DM, in contrast, reduced in skeletal muscle after acute exercise (28), congruous with the premise that *PGC-1α* DNA methylation plays a role in glucose homeostasis. On the other hand, Gillberg *et al.* (29) reported that *PGC-1α* promoter methylation was correlated with insulin sensitivity in a paradoxically positive manner.

Promoter methylation is one of the primary mechanisms that modulates transcription-factor binding, and increased DNA methylation silences gene transcription (23). In agreement with this notion, *PGC-1α* mRNA was lower in the liver and muscle of CG-IUGR rats, indicating that the promoter methylation is a possible epigenetic mechanism for controlling *PGC-1α* transcriptional activity. Interestingly, the mRNA content of *PGC-1α* was not significantly correlated with promoter DNA methylation level, possibly due to the complex regulating network, in which *PGC-1α* can be delicately tuned in both transcriptional and posttranslational manners responding to various metabolic cues (16). Many previous findings also suggest an unfavorable role of reduced *PGC-1α* expression for insulin sensitivity: the *PGC-1α* expression is decreased in the liver of nonalcoholic fatty liver disease patients (18) and adult rat offspring after exposure to a nutritional insult (30), as well as in islet (17) and skeletal muscle (27) from T2DM patients, and *PGC-1α* transcriptional activity is associated with insulin sensitivity (18,30). Besides, losing one allele of hepatic *PGC-1α* results in the chronic reduction of *PGC-1α* expression and impairs insulin signaling in mice (31). Taken together, an appropriate expression of *PGC-1α* is probably substantial for metabolic programing, and the reduced transcriptional activity of *PGC-1α* may contribute to metabolic-syndrome-related phenotype in adult CG-IUGR rats.

It has been well established that PGC-1α is a chief regulator of mitochondrial biogenesis and function (14). Mitochondrial dysfunction is closely linked to mitochondrial content, and mitochondrial deficiency is believed to impair insulin sensitivity, demonstrated in T2DM (27) and nonalcoholic fatty liver disease patients (18). Similarly, we observed that the mtDNA/nDNA ratio was reduced in the liver and muscle of CG-IUGR rats, indicative of attenuated mitochondrial content and impaired mitochondrial function. The mtDNA/nDNA ratio was inversely correlated with the methylation content of *PGC-1α* promoter in muscle and liver, and positively correlated with *PGC-1α* mRNA abundance in liver but not in muscle, indicating a possible tissue-specific effect of gene expression and DNA methylation of *PGC-1α* on the mitochondrial content.

Moreover, the mRNA abundances of other mitochondrial markers, PGC-1α-targeted genes involved in oxidative phosphorylation and regulation of mitochondrial DNA replications (16), were decreased in the liver and muscle of CG-IUGR rats, conceivably mediated by the alteration of *PGC-1α*.

PPAR-α, a receptor highly expressed in liver and muscle, plays an essential role in lipid metabolism (32). The functional interaction between *PGC-1α* and PPAR-α can stimulate lipid oxidation and decrease TG accumulation (32), while PPAR-γ may govern whole-body insulin sensitivity and lipid metabolism (33). In this study, the mRNA content of *PPAR-α*, *CD36*, and *PPAR-γ* was reduced in liver while only *PPAR-α* mRNA level was attenuated in the muscle of CG-IUGR rats, implicating a possible impairment of fatty acid oxidation at a different extent in the liver and muscle of GC-IUGR rats. The TG content of GC-IUGR adult rats was elevated in the liver tissue alone, and was positively correlated with the methylation of *PGC-1α*, suggesting that the modification in *PGC-1α* methylation may play an initial role in the alteration of fatty acid oxidation in the liver of CG-IUGR rats.

In our previous study, the CG-IUGR adult rats were found to have increased body weight and greater percentage of visceral fat (21), yet there was no significant difference in core temperature between the groups. This is in agreement with the observations in obese and lean humans (34). However, it does not necessarily mean that core temperature is immaterial to the promotion and maintenance of obesity in CG-IUGR rats. In fact, the association between body weight and body thermoregulation remains contestable. For example, before exercise, body temperature was higher in obese children (35), while another study found, in contrast, that obesity-prone dogs have lower core temperature than obesity-resistant dogs (36). In our study, the spontaneous physical activity also did not differ between the control and obese CG-IUGR rats; similarly, the diet-induced obese rat and the diet-resistant rat had no difference in spontaneous physical activity (37). However, after 29 d on a high-fat diet, obese rats decreased their spontaneous

Table 1. The primers used in quantitative PCR

Gene	Primers	Sequence from 5′ to 3′	Product length
PGC-1α	Forward	GTG CAG CCA AGA CTC TGT ATG G	121 bp
	Reverse	GTC CAG GTC ATT CAC ATC AAG TTC	
Cycs	Forward	CTA AAC ACC AGG ACG GAA CT	286 bp
	Reverse	CCA ATC AGG CAT GAA CAG	
Sdhd	Forward	GGC ATT GGA CAA GTG GTT	205 bp
	Reverse	GAG GCA AGG AGG CAT ACA	
Uqcrc1	Forward	TTG ACG TTG GCA GTC GCT AT	93 bp
	Reverse	CAG GAC GGT TCT TTG TTC CCT	
Atp5b	Forward	TTC TAC TAC GAA CCG CTC CC	113 bp
	Reverse	GCC GAT GAC TGC CAC AAT	
TFAM	Forward	CGC CTA AAG AAG AAA GCA CA	271 bp
	Reverse	GCC CAA CTT CAG CCA TTT	
NRF1	Forward	GTT TGA GTC TAA CCC ATC TAT CCG	98 bp
	Reverse	GCT GTC CCA CTC GTG TCG TAT	
PPAR-α	Forward	GGA ATT TGC CAA GGC TAT CCC	135 bp
	Reverse	GCG ATC AGC ATC CCG TCT TT	
CD36	Forward	AGA CTG GGA CCA TCG G	190 bp
	Reverse	CAT AAT GTA GGC TCA TCC AC	
CPT1A	Forward	GCG GCG TCC TCT TTG GT	126 bp
	Reverse	TGG TGC TGC GGC TCA TT	
CPT1B	Forward	GTT CAA CAC TAC ACG CAT CCC	121 bp
	Reverse	CGA GCC CTC ATA GAG CCA AA	
GAPDH	Forward	GCA CAG TCA AGG CTG AGA ATG	140 bp
	Reverse	GGT GGT GAA GAC GCC AGT A	

physical activity (37). Thus, we cannot exclude the possibility that CG-IUGR rats curtail their physical activity when faced a nutritional insult such as high-fat diet.

In conclusion, IUGR followed by postnatal accelerated growth programs an insulin-resistant phenotype, possibly through the alteration in DNA methylation and transcriptional activity of *PGC-1α*. The genetic and epigenetic modifications of *PGC-1α* possibly further mediate the reduction of mitochondrial content, the transcription of genes involved in fatty acid oxidation as well as oxidative phosphorylation, and the increment of hepatic TG accumulation, providing a potential mechanism linking early-life nutrition insult to long-term adverse metabolic consequences.

MATERIALS AND METHODS

Animal Model Establishment

A CG-IUGR rat model was established by maternal nutritional restriction and litter size reduction as described in our previous studies (20–22). Briefly, pregnant rats were randomly divided into two groups, the control group (AGA group) mothers received a standard rodent chow while the CG-IUGR group mothers were provided with 30% of normal intake during the entire gestational period. Mothers of both groups were fed *ad libitum* once the rat pups were delivered. The gestation length, sex ratio, litter size, and survival rates of the fetuses in both groups were similar. The litter size was reduced to five pups/litter at birth in the CG-IUGR group while eight pups/litter in the control group to ensure postnatal accelerated growth of the rats with IUGR. All pups were weaned after breastfeeding of 3 wk, and fed a standard chow thereafter. At the age of 8 wk, rats were fasten overnight before obtaining liver and skeletal muscle (vastus lateralis) tissues, which were immediately frozen in liquid nitrogen. For each assay, in each group, at least five rats from different litters were used. All rats were males, with the exception that blood was also sampled from two female rats for the fasting insulin assay. All animal procedures were conducted according to the guidelines of the Council for International Organizations of Medical Sciences, and with ethical approval from the Ethical Review Board of Animal Study Committee in Tongji Medical College, Huazhong University of Science and Technology, Wuhan, China.

Bisulfite Treatment of DNA and Pyrosequencing

Genomic DNA was extracted from the liver and muscle tissues using the DNeasy Blood & Tissue Kit (Qiagen GmbH, Hilden, Germany), and bisulfite conversion was conducted using the EZ DNA Methylation Gold kit (Zymo Research, Irvine, CA). A sequence starting 1,000 bp upstream from the *PGC-1α* transcription start site (TSS) was retrieved from the Transcriptional Start Sites Database (the University of Tokyo, Tokyo, Japan) with the following ID numbers: NM_031347; Archive EnsEMBL: Chromosome 14: 64,278,122-64,371,412; TSS: 64278115. And the sequence was also confirmed in UCSC Genome Bioinformatics Database (UCSC Genome Informatics Group, Santa Cruz, CA). Seven CpG sites in *PGC-1α* promoter were selected to analyze according to the previous studies (19,29) (**Figure 6**). Four primer assays covering the CpG sites of interest in the *PGC-1α* promoter were designed using the PyroMark Assay Design Software (version 2.0.1.15; Qiagen GmbH). Assay1 (forward primer: 5′-GAGGGGAATTTAAGAGTTTAGGGT-3′; reverse primer: 5′-ACTCCAAATCAACTATCTCCTTAACAATAA-3′; sequencing primer: 5′-GGTGTTGGGTTTGTTTA-3′) covered CpG sites located at −803 and −787 bp upstream from the *PGC-1α* TSS, assay2 (forward primer: 5′-AAATAAATGAGGTTGTTTGGTTGATT

AA-3′; reverse primer: 5′-CCATAAAATTCTTTTTTTTCTCCCTA TTAA-3′; sequencing primer: 5′-CCCTATTAAAAAAATATTTAAA AAC-3′) covered CpG site −582 bp upstream from the *PGC-1α* TSS, assay3 (forward primer: 5′-AAGGGTGTAGTTATTGT GTTAGTAATAGAG-3′; reverse primer: 5′-ACCTTTAAAAAACT TCAAACATCACACTAT-3′; sequencing primer: 5′-TGAGTTATT ATATGATTAGGGT-3′) covered CpG site −326 bp upstream from the *PGC-1α* TSS, and assay4 (forward primer: 5′-TTGGT GGTATTTAAAGTTGGTTTTAGTTAT-3′; reverse primer: 5′-CTCC CTTCTCCTATACAACTTAC-3′; sequencing primer: 5′-CCTATA CAACTTACTACTCA-3′) covered CpG sites −215, −186, and −178 bp upstream from the *PGC-1α* TSS. The bisulfite-modified DNA was amplified by touchdown PCR using ZymoTaq PreMix (Zymo Research). Biotinylated PCR products were immobilized on streptavidin-coated Sepharose beads (GE Healthcare Bio-Sciences AB, Uppsala, Sweden) to get single-stranded DNA templates. After the annealing of sequencing primers and preparation of PyroMark Gold Q96 Reagents (Qiagen GmbH), pyrosequencing reaction was carried out in a PyroMark Q96 ID instrument (Qiagen GmbH). The quantification (%) of cytosine methylation levels at each target CpG site of *PGC-1α* promoter was performed using the Pyrogram software (Qiagen GmbH), and data were subjected to quality control.

Real-Time Quantitative PCR

Total RNA was isolated from the liver and muscle tissues with TRIzol reagent (Life Technologies, Carlsbad, CA) following the manufacturer's protocol. After the assessment of RNA quantity and quality, RNA was reverse-transcribed using the First Strand cDNA Synthesis Kit (Thermo Scientific, Waltham, MA). The primers for real-time quantitative PCR (qPCR) of *PPAR-γ* were previously reported (38), and the other qPCR primers were designed using Primer Premier software (PREMIER Biosoft International, Palo Alto, CA, Version 5.0). The specificity of these primers was checked using Primer-BLAST. Primers details are provided in **Table 1**. All amplifications were performed in an ABI 7500 real-time PCR system (Life Technologies) with a 20-μl reaction mixture consisting of 0.3 μmol/l primers, 100 ng cDNA, and 10 μl 2× SYBR Green/ROX qPCR Master Mix (Thermo Scientific). Melting curve analysis and agarose gel electrophoresis were conducted to verify the specificity of qPCR products. *Glyceraldehyde 3-phosphate dehydrogenase (GAPDH)* was amplified as an internal control. Relative gene expression was analyzed by the comparative C(T) method.

Western Blot Analysis

The liver and muscle tissue proteins were extracted with radioimmunoprecipitation assay (RIPA) lysis buffer containing 1 mmol/l phenylmethylsulfonyl fluoride (PMSF) (Beyotime, Nantong, China). Lysates were fractionated on a 10% sodium dodecyl sulfate (SDS)-polyacrylamide gel and subsequently electroblotted onto polyvinyl difluoride (PVDF) membranes (EMD Millipore, Billerica, MA). After blocked in western blocking buffer (Beyotime), the membranes were incubated with primary antibodies including PI3K p85 (1:1,000 dilution; Cell Signaling Technology, Danvers, MA), Akt2 (1:1,000 dilution; Cell Signaling Technology), pS474-Akt2 (1:1,000 dilution; Abcam, Cambridge, UK), and GAPDH (1:5,000 dilution; Epitomics, Burlingame, CA) overnight at 4 °C. After washed with Tris-Buffered Saline plus Tween 20 (TBST) for 45 min, the membranes were probed with the IRDye 800CW secondary antibodies (1:25,000 dilution; LI-COR Biosciences, Lincoln, NE) for half an hour or horseradish-peroxidase-conjugated secondary antibodies (1:4,000; Jackson ImmunoResearch, West Grove, PA) for 1 h at 37 °C. The membranes were washed with Tris-Buffered Saline plus Tween 20 (TBST) for 1 h, followed by scanning with Odyssey Infrared Imaging System (LI-COR Biosciences) or developed using the enhanced chemiluminescence detection kit (Thermo Scientific). GAPDH was used as a protein-loading control.

Measurement of Mitochondria Content

The mitochondria content was presented as the mtDNA/nDNA ratio and determined as previously described (27). In short, a fragment located in *COX1* (NC_001665) was amplified with the primers forward: CAATTCCTACAGGCGTAAA and reverse: CAATGTCAAGGGATGAGTTAG for mDNA, while a fragment in *ACTB* (NC_005111) sequence was amplified with the primers forward: TAATGAGGCTGGTGATAAATGGC and reverse: GGGCAGGTGAGACTGTAAGGAT for nDNA. The amplifications were carried out in an ABI 7500 real-time PCR system (Life Technologies) with a 20-μl reaction mixture containing 80 ng of purified DNA, 1× SYBR Green/ROX qPCR Master Mix (Thermo Scientific) and 0.3 μmol/l of each primer. The specificity of amplification was confirmed by the melting curve analysis and agarose gel electrophoresis of the products. Each sample was measured in triplicate.

Plasma Insulin and Liver Tissue Triglyceride (TG) Measurement

Fasting plasma insulin was measured using an enzyme-linked immunosorbent assay (ELISA) kit (Mercodia AB, Uppasla, Sweden) according to the manufacture's instructions. The liver and muscle tissues were lyzed in RIPA buffer, and the TG content was determined using a colorimetric assay previously described (39). The TG level was expressed as milligram lipid per milligram of tissue protein.

Core Temperature and Spontaneous Physical Activity

The core body temperature was assessed rectally by a digital probe thermometer (Omron, Kyoto, Japan) following the method previously described (40). The spontaneous physical activity was recorded for 1 h in locomotion cages (45 cm × 45 cm) by using AniLab Software (AniLab Software & instruments, Ningbo, China) following the manufacturer's instructions.

Statistical Analysis

The data were expressed as mean ± SEM (n). The differences between two groups were determined by an independent-sample t-test. The correlation between the two variables was examined using Pearson correlation test. A strong correlation is considered if Pearson correlation coefficient (r) is >0.6. $P < 0.05$ (two-tailed) was considered statistically significant. The statistical analyses were performed with SPSS 16.0 software (SPSS, Chicago, IL).

ACKNOWLEDGMENTS

We thank Professors Kenneth McCormick and Gail Mick from the Department of Pediatrics, Endocrine Division, University of Alabama at Birmingham (UAB), Birmingham, AL, USA, for their assistance with the English language editing and manuscript composition.

STATEMENT OF FINANCIAL SUPPORT

This study was supported by the grant from the National Natural Science Foundation of China (No. 81170627) and Program for Changjiang Scholars and Innovative Research Team in University (PCSIRT1131).

Disclosure: The authors declare no conflict of interest.

REFERENCES

1. Barker DJ, Hales CN, Fall CH, Osmond C, Phipps K, Clark PM. Type 2 (non-insulin-dependent) diabetes mellitus, hypertension and hyperlipidaemia (syndrome X): relation to reduced fetal growth. Diabetologia 1993;36:62–7.
2. Hales CN, Barker DJ, Clark PM, et al. Fetal and infant growth and impaired glucose tolerance at age 64. BMJ 1991;303:1019–22.
3. Bhuiyan AR, Chen W, Srinivasan SR, Azevedo MJ, Berenson GS. Relationship of low birth weight to pulsatile arterial function in asymptomatic younger adults: the Bogalusa Heart Study. Am J Hypertens 2010;23:168–73.
4. Hernández MI, Mericq V. Metabolic syndrome in children born small-for-gestational age. Arq Bras Endocrinol Metabol 2011;55:583–9.
5. Mericq V. Low birth weight and endocrine dysfunction in postnatal life. Pediatr Endocrinol Rev 2006;4:3–14.
6. Roghair RD, Aldape G. Naturally occurring perinatal growth restriction in mice programs cardiovascular and endocrine function in a sex- and strain-dependent manner. Pediatr Res 2007;62:399–404.
7. Lim JS, Lee JA, Hwang JS, Shin CH, Yang SW. Non-catch-up growth in intrauterine growth-retarded rats showed glucose intolerance and increased expression of PDX-1 mRNA. Pediatr Int 2011;53:181–6.

8. Ong KK. Catch-up growth in small for gestational age babies: good or bad? Curr Opin Endocrinol Diabetes Obes 2007;14:30–4.
9. Ehrenkranz RA, Dusick AM, Vohr BR, Wright LL, Wrage LA, Poole WK. Growth in the neonatal intensive care unit influences neurodevelopmental and growth outcomes of extremely low birth weight infants. Pediatrics 2006;117:1253–61.
10. Casey PH, Whiteside-Mansell L, Barrett K, Bradley RH, Gargus R. Impact of prenatal and/or postnatal growth problems in low birth weight preterm infants on school-age outcomes: an 8-year longitudinal evaluation. Pediatrics 2006;118:1078–86.
11. Faienza MF, Brunetti G, Ventura A, et al. Nonalcoholic fatty liver disease in prepubertal children born small for gestational age: influence of rapid weight catch-up growth. Horm Res Paediatr 2013;79:103–9.
12. Berends LM, Fernandez-Twinn DS, Martin-Gronert MS, Cripps RL, Ozanne SE. Catch-up growth following intra-uterine growth-restriction programmes an insulin-resistant phenotype in adipose tissue. Int J Obes (Lond) 2013;37:1051–7.
13. Hermann GM, Miller RL, Erkonen GE, et al. Neonatal catch up growth increases diabetes susceptibility but improves behavioral and cardiovascular outcomes of low birth weight male mice. Pediatr Res 2009;66:53–8.
14. Heijmans BT, Tobi EW, Stein AD, et al. Persistent epigenetic differences associated with prenatal exposure to famine in humans. Proc Natl Acad Sci USA 2008;105:17046–9.
15. Plagemann A, Roepke K, Harder T, et al. Epigenetic malprogramming of the insulin receptor promoter due to developmental overfeeding. J Perinat Med 2010;38:393–400.
16. Fernandez-Marcos PJ, Auwerx J. Regulation of PGC-1α, a nodal regulator of mitochondrial biogenesis. Am J Clin Nutr 2011;93:884S–90.
17. Ling C, Del Guerra S, Lupi R, et al. Epigenetic regulation of PPARGC1A in human type 2 diabetic islets and effect on insulin secretion. Diabetologia 2008;51:615–22.
18. Sookoian S, Rosselli MS, Gemma C, et al. Epigenetic regulation of insulin resistance in nonalcoholic fatty liver disease: impact of liver methylation of the peroxisome proliferator-activated receptor γ coactivator 1α promoter. Hepatology 2010;52:1992–2000.
19. Brøns C, Jacobsen S, Nilsson E, et al. Deoxyribonucleic acid methylation and gene expression of PPARGC1A in human muscle is influenced by high-fat overfeeding in a birth-weight-dependent manner. J Clin Endocrinol Metab 2010;95:3048–56.
20. Zheng RD, Liao LH, Ye J, et al. Effects of SOCS 1/3 gene silencing on the expression of C/EBPα and PPARγ during differentiation and maturation of rat preadipocytes. Pediatr Res 2013;73:263–7.
21. Ye J, Zheng R, Wang Q, et al. Downregulating SOCS3 with siRNA ameliorates insulin signaling and glucose metabolism in hepatocytes of IUGR rats with catch-up growth. Pediatr Res 2012;72:550–9.
22. Liao L, Zheng R, Wang C, et al. The influence of down-regulation of suppressor of cellular signaling proteins by RNAi on glucose transport of intrauterine growth retardation rats. Pediatr Res 2011;69:497–503.
23. Suzuki MM, Bird A. DNA methylation landscapes: provocative insights from epigenomics. Nat Rev Genet 2008;9:465–76.
24. Gemma C, Sookoian S, Alvariñas J, et al. Maternal pregestational BMI is associated with methylation of the PPARGC1A promoter in newborns. Obesity (Silver Spring) 2009;17:1032–9.
25. Zeng Y, Gu P, Liu K, Huang P. Maternal protein restriction in rats leads to reduced PGC-1α expression via altered DNA methylation in skeletal muscle. Mol Med Rep 2013;7:306–12.
26. Pooya S, Blaise S, Moreno Garcia M, et al. Methyl donor deficiency impairs fatty acid oxidation through PGC-1α hypomethylation and decreased ER-α, ERR-α, and HNF-4α in the rat liver. J Hepatol 2012;57:344–51.
27. Barrès R, Osler ME, Yan J, et al. Non-CpG methylation of the PGC-1alpha promoter through DNMT3B controls mitochondrial density. Cell Metab 2009;10:189–98.
28. Barrès R, Yan J, Egan B, et al. Acute exercise remodels promoter methylation in human skeletal muscle. Cell Metab 2012;15:405–11.
29. Gillberg L, Jacobsen SC, Jacobsen S, et al. Does DNA methylation of PPARGC1A influence insulin action in first degree relatives of patients with type 2 diabetes? PLoS One 2013;8:e58384.
30. Burgueño AL, Cabrerizo R, Gonzales Mansilla N, Sookoian S, Pirola CJ. Maternal high-fat intake during pregnancy programs metabolic-syndrome-related phenotypes through liver mitochondrial DNA copy number and transcriptional activity of liver PPARGC1A. J Nutr Biochem 2013;24:6–13.
31. Estall JL, Kahn M, Cooper MP, et al. Sensitivity of lipid metabolism and insulin signaling to genetic alterations in hepatic peroxisome proliferator-activated receptor-gamma coactivator-1alpha expression. Diabetes 2009;58:1499–508.
32. Burri L, Thoresen GH, Berge RK. The Role of PPARα Activation in Liver and Muscle. PPAR Res 2010;2010:.
33. Abbas A, Blandon J, Rude J, Elfar A, Mukherjee D. PPAR-γ agonist in treatment of diabetes: cardiovascular safety considerations. Cardiovasc Hematol Agents Med Chem 2012;10:124–34.
34. Heikens MJ, Gorbach AM, Eden HS, et al. Core body temperature in obesity. Am J Clin Nutr 2011;93:963–7.
35. Leites GT, Sehl PL, Cunha Gdos S, Detoni Filho A, Meyer F. Responses of obese and lean girls exercising under heat and thermoneutral conditions. J Pediatr 2013;162:1054–60.
36. Hynd PI, Czerwinski VH, McWhorter TJ. Is propensity to obesity associated with the diurnal pattern of core body temperature? Int J Obes (Lond) 2014;38:231–5.
37. Novak CM, Kotz CM, Levine JA. Central orexin sensitivity, physical activity, and obesity in diet-induced obese and diet-resistant rats. Am J Physiol Endocrinol Metab 2006;290:E396–403.
38. Zhu C, Zhang X, Qiao H, et al. The intrinsic PEDF is regulated by PPARγ in permanent focal cerebral ischemia of rat. Neurochem Res 2012;37:2099–107.
39. Qiu BY, Turner N, Li YY, et al. High-throughput assay for modulators of mitochondrial membrane potential identifies a novel compound with beneficial effects on db/db mice. Diabetes 2010;59:256–65.
40. Vanattou-Saïfoudine N, McNamara R, Harkin A. Mechanisms mediating the ability of caffeine to influence MDMA ('Ecstasy')-induced hyperthermia in rats. Br J Pharmacol 2010;160:860–77.